

Supplemental Material for
Contact Angle of An Evaporating Droplet of Binary Solution on a
Super Wetting Surface

Mengmeng Wu,^{1,2} Masao Doi,^{1,2} and Xingkun Man^{1,2,*}

¹*Center of Soft Matter Physics and its Applications,
Beihang University, Beijing 100191, China*

²*School of Physics, Beihang University, Beijing 100191, China*

A. Detailed derivation of the model

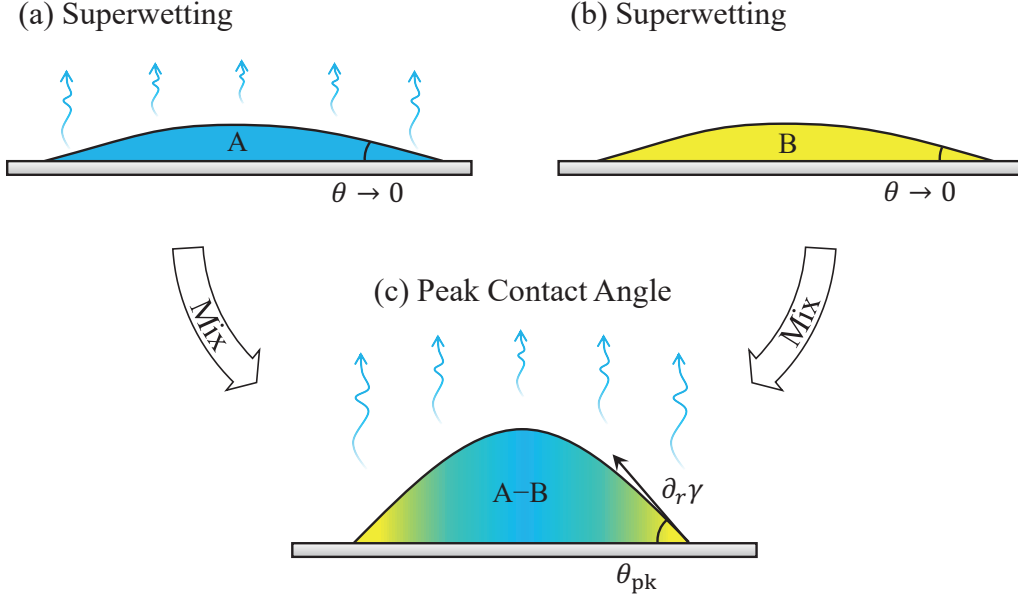


FIG. 1. Schematic pictures of droplet with (a) single volatile component, (b) single nonvolatile component, and (c) mixture of the two components. Both of the two components are super-wetting on the substrate, and the surface tension of the volatile component is larger than the nonvolatile one. The nonuniform evaporation of the binary droplet in (c) causes an inward surface tension gradient, which induces a peak contact angle θ_{pk} during evaporation.

Consider a droplet placed on a substrate which is a solution made of volatile component A and non-volatile component B, as shown in Fig. 1. We assume that the droplet contact angle is small and that the surface profile is approximated by a parabolic function

$$h(r, t) = H(t) \left[1 - \frac{r^2}{R^2(t)} \right], \quad (\text{A.1})$$

where $H(t)$ is the height at the droplet center and $R(t)$ is the radius of the droplet base. Then, the droplet volume $V(t)$ is given by

$$V(t) = \frac{\pi}{2} H(t) R^2(t). \quad (\text{A.2})$$

The contact angle $\theta(t)$ is given by $-\partial h(r, t)/\partial r$ at $r = R(t)$. Eqs. (A.1) and (A.2) then give

$$\theta(t) = \frac{4V(t)}{\pi R^3(t)}. \quad (\text{A.3})$$

* manxk@buaa.edu.cn

Let $J(r)$ be the evaporation rate (the liquid volume evaporating to air per unit time per

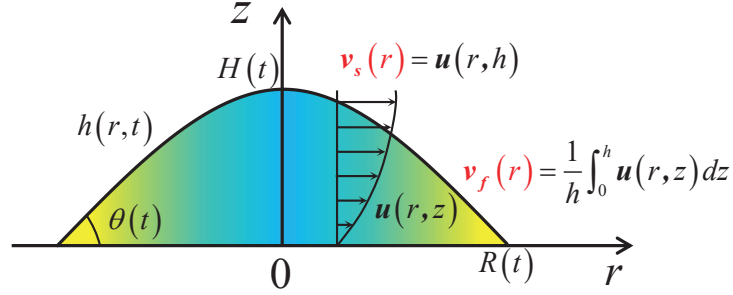


FIG. 2. Schematic of the height averaged fluid velocity $v_f(r)$ and the fluid velocity at the liquid/vapor interface $v_s(r)$ (side view). The fluid flow velocity is $u(r, z)$, the radius of the contact line is R , the height of the droplet at the center is H , the contact angle is θ , and the profile of the droplet liquid-vapor interface is $h(r)$.

unit surface area) at point r . The volume change rate is related to J as

$$\dot{V}(t) = - \int_0^R 2\pi r J dr. \quad (\text{A.4})$$

We assume the evaporation rate of the nonvolatile component B equals to zero, and the evaporation rate of the binary droplet on a substrate is proportional to the concentration of the volatile component A, which is given by the following form [1–3]

$$J(r) = J_A [C(r) - RH], \quad (\text{A.5})$$

where $C(r)$ is the height-averaged mass fraction of the volatile component in the droplet, RH is the relative humidity of A component, and J_A is the evaporation rate of pure droplet having the same volume and base radius of the solution droplet when $RH = 0$. Here we reduced our problems to the ideal case of Raoult's law. The explicit form of J_A is written by [1, 4, 5]

$$J_A = \frac{\theta_0 R_0^2}{4R\tau_{\text{ev}}}, \quad (\text{A.6})$$

where $\tau_{\text{ev}} = -V_0/\dot{V}_0$ is the characteristic evaporation time for the pure A droplet when $RH = 0$ with \dot{V}_0 being a given constant, and V_0 , θ_0 and R_0 are the initial values of $V(t)$, $\theta(t)$ and $R(t)$, respectively. The liquid/vapor surface tension γ of the solution depends on the composition in the solution. We assume a linear dependence on $C(r)$ [2],

$$\gamma(r) = \gamma_A C + \frac{\gamma_A}{\gamma_{\text{re}}} (1 - C), \quad (\text{A.7})$$

where $\gamma_{re} = \gamma_A/\gamma_B$, γ_A and γ_B are the surface tensions of pure A and B components, respectively.

In this model, we use the Onsager principle to determine the time evolution of the contact radius \dot{R} and the contact angle $\dot{\theta}$ by minimizing the Rayleighian defined by [6]

$$\mathcal{R} = \dot{F} + \Phi, \quad (\text{A.8})$$

where \dot{F} is the time change rate of the free energy of the system, and Φ is the energy dissipation function.

The change rate of free energy \dot{F} has two parts: the interface free energy contribution \dot{F}_C and the Marangoni flow contribution \dot{F}_M . We assume that the droplet size is less than the capillary length and the droplet is nearly flat $|h'| \ll 1$, then the sum of the interfacial energy is written as

$$\begin{aligned} F_C &= \int_0^R 2\pi r \left[\gamma(r) \sqrt{1 + h'^2(r)} - \gamma_A \cos \theta_{eA} \right] dr \\ &= \int_0^R 2\pi r \left[\gamma(r) \left(1 + \frac{1}{2} h'^2(r) \right) - \gamma_A \left(1 - \frac{1}{2} \theta_{eA}^2 \right) \right] dr. \end{aligned} \quad (\text{A.9})$$

where the surface tension γ of solution depends on the composition in the solution, and θ_{eA} is the equilibrium contact angle for A component, $\gamma_A \cos \theta_{eA} = \gamma_{SV} - \gamma_{LS}$. Here γ_{SV} and γ_{LS} are the surface tension of the substrate/vapor and the liquid/substrate interfaces, respectively. Therefore, \dot{F}_C has the form

$$\begin{aligned} \dot{F}_C &= \int_0^R 2\pi r \left[\gamma(r) h'(r) \dot{h}'(r) + \dot{C}(r) \frac{\partial \gamma(r)}{\partial C(r)} \left(1 + \frac{h'^2(r)}{2} \right) \right] dr \\ &\quad + 2\pi R \dot{R} \left[\gamma(R) \left(1 + \frac{h'^2(R)}{2} \right) - \gamma_A \left(1 - \frac{1}{2} \theta_{eA}^2 \right) \right], \end{aligned} \quad (\text{A.10})$$

while the Marangoni flow contribution to the change rate of free energy [7],

$$\dot{F}_M = - \int_0^R 2\pi r \mathbf{v}_s \frac{\partial \gamma}{\partial r} dr, \quad (\text{A.11})$$

where \mathbf{v}_s is the fluid velocity at the liquid-vapor interface.

We use the lubrication approximation to calculate the dissipation function. Therefore, the energy dissipation Φ taking place in the system is

$$\Phi = \frac{\eta}{2} \int_0^R \int_0^h 2\pi r \left(\frac{\partial \mathbf{u}}{\partial z} \right)^2 dz dr. \quad (\text{A.12})$$

where η is the viscosity of the fluid, and \mathbf{u} is the fluid velocity inside the droplet as shown in Fig. 2.

According to the lubrication theory, the general expression of the fluid velocity \mathbf{u} as a function of z is

$$\mathbf{u}(r, z, t) = (Az^2 + Bz + C) \mathbf{i}. \quad (\text{A.13})$$

The boundary conditions of \mathbf{u} are,

$$\begin{aligned} \mathbf{u}(r, 0, t) &= 0, \\ \mathbf{u}(r, h, t) &= \mathbf{v}_s(r, t), \end{aligned} \quad (\text{A.14})$$

where $\mathbf{v}_s(r, t)$ is the fluid velocity at the liquid-vapor interface. To simplify the calculation of Φ , we define a height averaged fluid velocity as

$$\mathbf{v}_f(r, t) = \frac{1}{h} \int_0^h \mathbf{u}(r, z, t) dz. \quad (\text{A.15})$$

The definitions of \mathbf{v}_f and \mathbf{v}_s are schematically shown in Fig. 2, $\mathbf{v}_f(r)$ is the height averaged fluid velocity at position r . Then, $\mathbf{u}(r, z, t)$ becomes

$$\mathbf{u} = \frac{3(\mathbf{v}_s - 2\mathbf{v}_f)}{h^2} z^2 + \frac{2(3\mathbf{v}_f - \mathbf{v}_s)}{h} z. \quad (\text{A.16})$$

Combining Eqs. (A.12) and (A.16), the energy dissipation caused by the fluid flow inside the droplet becomes

$$\Phi = \int_0^R 2\pi r \frac{\eta}{2h} \left[12 \left(\mathbf{v}_f - \frac{\mathbf{v}_s}{2} \right)^2 + \mathbf{v}_s^2 \right] dr, \quad (\text{A.17})$$

Minimizing the Rayleighian, $\mathcal{R} = \Phi + \dot{F}$, with respect to $\mathbf{v}_s(r)$ leading to

$$\mathbf{v}_s = \frac{3}{2} \mathbf{v}_f + \frac{h}{4\eta} \frac{\partial \gamma}{\partial r}. \quad (\text{A.18})$$

The velocity v_f and the time change rate of concentration \dot{C} are obtained from the mass conservation equation. The liquid volume conservation equation is written as

$$\dot{h} = -\frac{1}{r} \frac{\partial (rv_f h)}{\partial r} - J. \quad (\text{A.19})$$

Since $h(r, t)$ is given by Eq. (A.1), \dot{h} is expressed as a function of \dot{R} and \dot{H} . Therefore, by integrating Eq. (A.19), the height averaged fluid velocity $v_f(r)$ has a form

$$v_f = r \frac{\dot{R}}{R} - \left(\frac{r}{2V} + \frac{r^3}{2\pi R^4 h} \right) \dot{V} - \frac{1}{rh} \int_0^r r' J dr'. \quad (\text{A.20})$$

The conservation equation for the volatile component is written as

$$\frac{\partial(Ch)}{\partial t} = -\frac{1}{r} \frac{\partial(rv_f Ch)}{\partial r} - J, \quad (\text{A.21})$$

where we have ignore the diffusion of each component. Combining Eqs. (A.19) and (A.21), we obtain the evolution equation of the volatile component concentration,

$$\frac{\partial C}{\partial t} = -v_f \frac{\partial C}{\partial r} - \frac{J}{h} (1 - C). \quad (\text{A.22})$$

Inserting Eqs. (A.1), (A.2), (A.3), and (A.7) into Eq. (A.10), the time change rate of the interfacial free energy \dot{F}_C becomes

$$\begin{aligned} \dot{F}_C = & \int_0^R 2\pi r^3 [(\gamma_A - \gamma_B) C + \gamma_B] \left(\frac{16V}{\pi^2 R^8} \dot{V} - \frac{64V^2}{\pi^2 R^9} \dot{R} \right) dr - 2\pi R \dot{R} \gamma_A \left(1 - \frac{1}{2} \theta_{eA}^2 \right) \\ & + \int_0^R 2\pi r \dot{C} (\gamma_A - \gamma_B) \left(1 + \frac{r^2 \theta^2}{2R^2} \right) dr + 2\pi R \dot{R} [(\gamma_A - \gamma_B) C(R) + \gamma_B] \left(1 + \frac{\theta^2}{2} \right). \end{aligned} \quad (\text{A.23})$$

Inserting the expression of v_s and v_f into Eq. (A.11), \dot{F}_M is calculated as

$$\begin{aligned} \dot{F}_M = & - \int_0^R 3\pi r^2 (\gamma_A - \gamma_B) \frac{\partial C}{\partial r} \left[\frac{\dot{R}}{R} - \left(\frac{1}{2V} + \frac{r^2}{2\pi R^4 h} \right) \dot{V} - \frac{1}{2\pi r^2 h} \int_0^r r' J dr' \right] dr \\ & - \int_0^R \frac{\pi h r}{2\eta} (\gamma_A - \gamma_B)^2 \left(\frac{\partial C}{\partial r} \right)^2 dr. \end{aligned} \quad (\text{A.24})$$

Moreover, inserting the expression of v_s and v_f into Eq. (A.17), Φ is calculated as

$$\Phi = \int_0^R \frac{\pi \eta r}{h} \left[3r^2 \left(\frac{\dot{R}}{R} - \frac{\dot{V}}{2V} - \frac{r^2 \dot{V}}{2\pi R^4 h} - \frac{1}{r^2 h} \int_0^r r' J dr' \right)^2 + \frac{h^2 (\gamma_A - \gamma_B)^2}{4\eta^2} \left(\frac{\partial C}{\partial r} \right)^2 \right] dr. \quad (\text{A.25})$$

The Onsager principle states that \dot{R} is determined by the condition $\partial \mathcal{R} / \partial \dot{R} = 0$, and $\mathcal{R} = \dot{F} + \Phi$. Using Eq. (A.23), $\partial \dot{F}_C / \partial \dot{R}$ is writing as follows,

$$\begin{aligned} \frac{\partial \dot{F}_C}{\partial \dot{R}} = & - \int_0^R \frac{8\pi \theta^2 r^3}{R^3} [(\gamma_A - \gamma_B) C + \gamma_B] dr + \int_0^R 2\pi r \frac{\partial \dot{C}}{\partial \dot{R}} (\gamma_A - \gamma_B) \left(1 + \frac{r^2 \theta^2}{2R^2} \right) dr \\ & + 2\pi R [(\gamma_A - \gamma_B) C(R) + \gamma_B] \left(1 + \frac{\theta^2}{2} \right) - 2\pi R \gamma_A \left(1 - \frac{1}{2} \theta_{eA}^2 \right). \end{aligned} \quad (\text{A.26})$$

By Eqs. (A.20) and (A.22), we have the following expression of $\partial \dot{C} / \partial \dot{R}$,

$$\frac{\partial \dot{C}}{\partial \dot{R}} = -\frac{r}{R} \frac{\partial C}{\partial r}. \quad (\text{A.27})$$

Inserting Eq. (A.27) into Eq. (A.26), $\partial\dot{F}_C/\partial\dot{R}$ has the form,

$$\begin{aligned} \frac{\partial\dot{F}_C}{\partial\dot{R}} = & - \int_0^R \frac{8\pi\theta^2 r^3}{R^3} (\gamma_A - \gamma_B) C dr - \int_0^R \frac{2\pi r^2}{R} \frac{\partial C}{\partial r} (\gamma_A - \gamma_B) \left(1 + \frac{r^2\theta^2}{2R^2}\right) dr \\ & - 2\pi\gamma_B\theta^2 R + 2\pi R [(\gamma_A - \gamma_B) C(R) + \gamma_B] \left(1 + \frac{\theta^2}{2}\right) - 2\pi R\gamma_A \left(1 - \frac{1}{2}\theta_{eA}^2\right). \end{aligned} \quad (\text{A.28})$$

Using integration by parts, this can be rewritten as,

$$\frac{\partial\dot{F}_C}{\partial\dot{R}} = \int_0^R 4\pi (\gamma_A - \gamma_B) \frac{Cr}{R} \left(1 - \frac{r^2\theta^2}{R^2}\right) dr - 2\pi R (\gamma_A - \gamma_B) - \pi R (\gamma_B\theta^2 - \gamma_A\theta_{eA}^2) \quad (\text{A.29})$$

Then the expression of $\partial\dot{F}_M/\partial\dot{R}$ can be obtained from Eq. (A.24),

$$\begin{aligned} \frac{\partial\dot{F}_M}{\partial\dot{R}} = & - \int_0^R \frac{3\pi r^2}{R} (\gamma_A - \gamma_B) \frac{\partial C}{\partial r} dr \\ = & \int_0^R 6\pi (\gamma_A - \gamma_B) \frac{Cr}{R} dr - 3\pi (\gamma_A - \gamma_B) RC(R). \end{aligned} \quad (\text{A.30})$$

Similarly, $\partial\Phi/\partial\dot{R}$ is obtained from Eq. (A.25),

$$\begin{aligned} \frac{\partial\Phi}{\partial\dot{R}} = & \int_0^R \frac{6\pi\eta r^3}{hR} \left(\frac{\dot{R}}{R} - \frac{\dot{V}}{2V} - \frac{r^2\dot{V}}{2\pi R^4 h} - \frac{1}{r^2 h} \int_0^r r' J dr' \right) dr \\ = & \int_0^R \frac{6\pi\eta r^3}{hR} \left(\frac{\dot{R}}{R} - \frac{\dot{V}}{2V} - \frac{r^2\dot{V}}{2\pi R^4 h} + \frac{\dot{V}}{2\pi r^2 h} + \frac{1}{r^2 h} \int_r^R r' J dr' \right) dr. \end{aligned} \quad (\text{A.31})$$

Inserting Eqs. (A.1), (A.5) and (A.6) into Eq. (A.31), $\partial\Phi/\partial\dot{R}$ is calculated as,

$$\frac{\partial\Phi}{\partial\dot{R}} = \frac{3\pi^2\eta\alpha R^4}{2V} \dot{R} + \frac{3\pi^2\eta R^5 \dot{V}}{8V^2} + \frac{3\pi\eta\theta_0 R_0^2}{2\tau_{ev} R^2} \int_0^R \frac{r}{h^2} \left[\int_r^R r' (C - RH) dr' \right] dr, \quad (\text{A.32})$$

where $\alpha = \ln(R/2\epsilon) - 1$ is a parameter which is regarded as constant in the subsequent analysis [5].

Combining Eqs. (A.8), (A.29), (A.30), and (A.32), we have the evolution equations of the droplet

$$\begin{aligned} \tau_{ev} \dot{R} = & \frac{(\gamma_{re} - 1) \theta V_0^{\frac{1}{3}}}{3\gamma_{re} \alpha k_{ev}} \left[\int_0^R C \frac{r}{R^2} \left(\frac{2r^2\theta^2}{R^2} - 5 \right) dr + \frac{\theta^2 - \gamma_{re}\theta_{eA}^2}{2(\gamma_{re} - 1)} + \frac{3}{2} C(R) + 1 \right] \\ & - \frac{R\dot{V}\tau_{ev}}{4\alpha V} - \frac{\theta\theta_0 R_0^2}{4\alpha R^3} \int_0^R \frac{r}{h^2} \left[\int_r^R r' (C - RH) dr' \right] dr, \end{aligned} \quad (\text{A.33})$$

where $k_{ev} = \tau_{re}/\tau_{ev}$ is the evaporation rate parameter, the character relaxation time τ_{re} is defined by $\tau_{re} = \eta V_0^{\frac{1}{3}}/\gamma_A$.

Since $\dot{\theta}$ is related to \dot{V} by (see Eq. (A.3)),

$$\dot{\theta} = \theta \frac{\dot{V}}{V} - 3\theta \frac{\dot{R}}{R}. \quad (\text{A.34})$$

Eq. (A.33) gives the following time evolution equation for θ ,

$$\begin{aligned} \tau_{\text{ev}} \dot{\theta} = & \frac{(\gamma_{\text{re}} - 1) \theta^2 V_0^{\frac{1}{3}}}{\gamma_{\text{re}} \alpha k_{\text{ev}} R} \left[\int_0^R C \frac{r}{R^2} \left(5 - \frac{2r^2 \theta^2}{R^2} \right) dr - \frac{\theta^2 - \gamma_{\text{re}} \theta_{eA}^2}{2(\gamma_{\text{re}} - 1)} - \frac{3}{2} C(R) - 1 \right] \\ & + \frac{\theta \dot{V} \tau_{\text{ev}}}{V} \left(1 + \frac{3}{4\alpha} \right) + \frac{3\theta^2 \theta_0 R_0^2}{4\alpha R^4} \int_0^R \frac{r}{h^2} \left[\int_r^R r' (C - RH) dr' \right] dr. \end{aligned} \quad (\text{A.35})$$

It is worth noting that when C is set to 1, Eqs. (A.33) and (A.35) reduce to the model of single component droplet cases. When $C_0 = 1$, Eq. (A.33) can be reduced to

$$\begin{aligned} \tau_{\text{ev}} \dot{R} = & \frac{(\gamma_{\text{re}} - 1) \theta V_0^{\frac{1}{3}}}{3\gamma_{\text{re}} \alpha k_{\text{ev}}} \left[\frac{\theta^2 - 5}{2} + \frac{\theta^2 - \gamma_{\text{re}} \theta_{eA}^2}{2(\gamma_{\text{re}} - 1)} + \frac{5}{2} \right] - \frac{R \dot{V} \tau_{\text{ev}}}{4\alpha V} \\ & - \frac{\theta \theta_0 R_0^2}{8\alpha R^3} (1 - RH) \int_0^R \frac{r (R^2 - r^2)}{h^2} dr. \end{aligned} \quad (\text{A.36})$$

Inserting the parabolic form of $h(r, t)$ into Eq. (A.36) and integrating the last term, we have

$$\tau_{\text{ev}} \dot{R} = \frac{\theta V_0^{\frac{1}{3}}}{6\alpha k_{\text{ev}}} (\theta^2 - \theta_{eA}^2) - \frac{R \dot{V} \tau_{\text{ev}}}{4\alpha V} - \frac{\theta \theta_0 R_0^2 R}{16\alpha H^2} (1 - RH) (\alpha + 1). \quad (\text{A.37})$$

The last term of Eq. (A.37) can be written as a linear function of J_A by using the definition in Eq. (A.6),

$$\tau_{\text{ev}} \dot{R} = \frac{\theta V_0^{\frac{1}{3}}}{6\alpha k_{\text{ev}}} (\theta^2 - \theta_{eA}^2) - \frac{R \dot{V} \tau_{\text{ev}}}{4\alpha V} - \frac{\tau_{\text{ev}} \theta R^2 J_A}{4\alpha H^2} (1 - RH) (\alpha + 1). \quad (\text{A.38})$$

Inserting Eqs. (A.4) and (A.5) into Eq. (A.38), then the last term of Eq. (A.38) can be written as a linear function of \dot{V}

$$\tau_{\text{ev}} \dot{R} = \frac{\theta V_0^{\frac{1}{3}}}{6\alpha k_{\text{ev}}} (\theta^2 - \theta_{eA}^2) - \frac{R \dot{V} \tau_{\text{ev}}}{4\alpha V} + \frac{\tau_{\text{ev}} \theta \dot{V}}{4\pi \alpha H^2} (\alpha + 1). \quad (\text{A.39})$$

Based on Eqs. (A.2) and (A.3), the volume of droplet can be written as, $V = \pi H^2 R / \theta$. Then inserting such form of V into Eq. (A.39), the equation of $\dot{R}(t)$ for a drying single-component droplet is obtained as

$$\tau_{\text{ev}} \dot{R} = \frac{\theta V_0^{\frac{1}{3}}}{6\alpha k_{\text{ev}}} (\theta^2 - \theta_{eA}^2) + \frac{\tau_{\text{ev}} R \dot{V}}{4V}, \quad (\text{A.40})$$

which is consistent with the previous evolution equation of contact radius R for evaporating pure droplets [5]. Inserting Eq. (A.40) into (A.34), the time evolution equation of the droplet contact angle, $\dot{\theta}$, for a drying single-component droplet is written as

$$\tau_{\text{ev}} \dot{\theta} = \frac{\theta^2 V_0^{\frac{1}{3}}}{2\alpha k_{\text{ev}} R} (\theta_{eA}^2 - \theta^2) + \frac{\tau_{\text{ev}} \theta \dot{V}}{4V}. \quad (\text{A.41})$$

B. Comparison with experimental results when $\gamma_{re} < 1$

Our model is also suitable for the case of $\gamma_{re} < 1$. As an extension of the paper, we discuss the shape evolution of a drying binary droplet when $\gamma_{re} < 1$. Based on the Young's equation, the relationship between the equilibrium contact angle of pure A and B droplet, θ_{eA} and θ_{eB} , can be written as, $\cos \theta_{eB} = \gamma_{re} \cos \theta_{eA}$. In order to make the model more convenient to use in the case of $\gamma_{re} < 1$, we replace θ_{eA} by θ_{eB} in the evolution equations. Also, for comparing with experiments [8], we assume both of the two components can evaporate and introduce a relative evaporation rate parameter into the present theory model, $J_{re} = J_A/J_B$, where J_B is the evaporation rate for pure B droplet in dry ambient air, $RH_B = 0$. Then the evaporation rate becomes,

$$J(r) = J_A \left[C(r) - RH + \frac{1-C}{J_{re}} \right]. \quad (\text{A.42})$$

With the modified definition of J in Eq. (A.5), the volume change rate \dot{V} becomes

$$\dot{V}(t) = - \int_0^R 2\pi r J_A \left[C(r) - RH + \frac{1-C}{J_{re}} \right] dr, \quad (\text{A.43})$$

and the height averaged velocity $v_f(r)$ has a new form

$$v_f = r \frac{\dot{R}}{R} - \left(\frac{r}{2V} + \frac{r^3}{2\pi R^4 h} \right) \dot{V} - \frac{1}{rh} \int_0^r J_A r' \left[C(r) - RH + \frac{1-C}{J_{re}} \right] dr'. \quad (\text{A.44})$$

Then the time change rate of the concentration of volatile component $\dot{C}(r)$ becomes,

$$\dot{C} = -v_f \frac{\partial C}{\partial r} - \frac{J_A}{J_{re} h} [J_{re} (C(r) - RH) - C] [1 - C(r)]. \quad (\text{A.45})$$

Then, inserting the new \dot{V} , \dot{C} , and $v_f(r)$ into the dissipation function Φ , and the time change rate of free energy, \dot{F} , results in a new Rayleighian function. Then, we repeat the same minimization process to the Rayleighian and replace θ_{eA} by θ_{eB} , leading to a new evolution equation of the contact radius, $R(t)$,

$$\begin{aligned} \tau_{ev} \dot{R} = & \frac{(\gamma_{re} - 1) \theta V_0^{\frac{1}{3}}}{3\gamma_{re} \alpha k_{ev}} \left[\int_0^R C \frac{r}{R^2} \left(\frac{2r^2 \theta^2}{R^2} - 5 \right) dr + \frac{\theta^2 - \theta_{eB}^2}{2(\gamma_{re} - 1)} + \frac{3}{2} C(R) \right] - \frac{R \dot{V} \tau_{ev}}{4\alpha V} \\ & - \frac{\theta \theta_0 R_0^2}{4\alpha R^3} \int_0^R \frac{r}{h^2} \left[\int_r^R r' \left(C + \frac{1-C}{J_{re}} - RH \right) dr' \right] dr, \end{aligned} \quad (\text{A.46})$$

The evolution equation of the contact angle $\theta(t)$ becomes

$$\begin{aligned} \tau_{ev} \dot{\theta} = & \frac{(\gamma_{re} - 1) \theta^2 V_0^{\frac{1}{3}}}{\gamma_{re} \alpha k_{ev} R} \left[\int_0^R C \frac{r}{R^2} \left(5 - \frac{2r^2 \theta^2}{R^2} \right) dr - \frac{\theta^2 - \theta_{eB}^2}{2(\gamma_{re} - 1)} - \frac{3}{2} C(R) \right] \\ & + \frac{\theta \dot{V} \tau_{ev}}{V} \left(1 + \frac{3}{4\alpha} \right) + \frac{3\theta^2 \theta_0 R_0^2}{4\alpha R^4} \int_0^R \frac{r}{h^2} \left[\int_r^R r' \left(C + \frac{1-C}{J_{re}} - RH \right) dr' \right] dr. \end{aligned} \quad (\text{A.47})$$

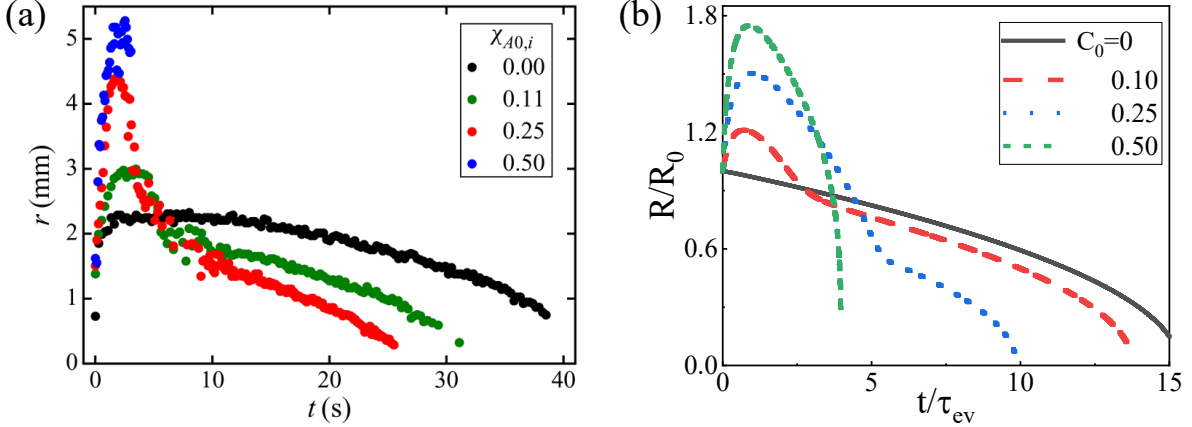


FIG. 3. (a) Evolution of droplet contact radius, r , of an evaporating ethanol/water droplet on heated substrate (70°C) for various initial concentration of ethanol, $\chi_{A0,i}$. Reprinted with the permission from Reference [8]. Copyright (2020) Cambridge University Press. (b) Corresponding theoretical results calculated by our theory model. $R(t)/R_0$ is the droplet contact radius, and C_0 is the initial concentration for the volatile A component, which is consistent with $\chi_{A0,i}$ in (a). All calculations are done for $\theta_0 = 0.4$, $RH = 0$, $\theta_e^B = 0.4$, and $\epsilon = 10^{-7}$. All the other parameters used for the calculation are given in the experimental parameters and theoretical framework of Reference [8].

Williams et al. [8] studied the evaporation of ethanol/water droplet on a high energy substrate, and found that increasing the initial ethanol concentration ($\chi_{A0,i}$) can enhance the droplet spreading, resulting in a larger maximum contact radius and shorter overall droplet lifetime, as shown in Figure 3(a). The enhanced spreading of droplet radius is explained by the fact that when $\chi_{A0,i}$ increases, the initial liquid/vapor surface tension decreases, and also the surface tension gradient from the apex to the contact line increases. Both effects enhance the spreading of contact line.

In order to compare with this finding, we carefully set values of parameters used in our model according to real experimental values used in [8]. We calculated the total evaporation rate, \dot{V}_0 , of a pure water droplet by using the data in Figure (11) of [8]. Then, we obtained the characteristic evaporation time of water droplet, $\tau_{ev}^B \approx 0.24\text{s}$ ($\tau_{ev} = -V_0/\dot{V}_0$). According to Eqs. (2.12) and (2.13) in [8], we obtained the ratio of evaporation rate between ethanol (J_A) and pure water (J_B) as $J_{re} = J_A/J_B \approx 10.26$. Combing the two values of τ_{ev} and J_{re} , we

obtained the characteristic evaporation time of ethanol, $\tau_{\text{ev}}^A = \tau_{\text{ev}}^B/10.26 \approx 0.023\text{s}$, which was used as the scale time in our model. In addition, Table 1 and Eq. (2.2) of [8] give the values of the surface tension of ethanol (γ_A) and water (γ_B), which are $\gamma_A \approx 2.24 \times 10^{-2}\text{Nm}^{-1}$ and $\gamma_B \approx 6.61 \times 10^{-2}\text{Nm}^{-1}$, respectively. Then, the surface tension ratio of the faster evaporation component over the slower one is $\gamma_{\text{re}} \approx 0.34$. Finally, with the values of the initial volume V_0 , viscosity η_A , γ_A and τ_{ev}^A , the evaporation rate parameter $k_{\text{ev}} = \eta_A V_0^{1/3}/(\gamma_A \tau_{\text{ev}}^A)$ of our present model has a value $k_{\text{ev}} \approx 1.88 \times 10^{-3}$. The calculated time dependent contact radius from our model is shown in Figure 3 (b) for various initial concentration of the more volatile component, C_0 . It is clear that when C_0 increases from 0 to 0.3, the droplet spreading is enhanced which is qualitatively consistent with the experimental results. The main reason of this phenomenon is the same as the explanations in [8], which is due to the enhanced Marangoni effects induced by the inhomogeneous surface tension.

C. Effects of the evaporation rate k_{ev}

In our model, the evaporation rate is determined by both k_{ev} and RH . The larger value of k_{ev} or smaller value of RH represent the faster evaporation rate. Figure 4 (a) shows the effect of k_{ev} on the time variation of the contact angle $\theta(t)$, and Figure 4(b) is the corresponding time evolution of the contact radius $R(t)$. When the evaporation rate is relatively large ($k_{\text{ev}} = 0.01$), the contact angle decreases monotonically in time. When k_{ev} decreases to 0.005, $\theta(t)$ starts to have a maximum value (i.e. a peak contact angle θ_{pk} appears). The maximum value increases when k_{ev} decreases. Meanwhile, the contact radius $R(t)$ shows the decreasing-increasing transition as k_{ev} decrease as it is shown in Figure 4(b). An important point here is that $\overline{\partial C/\partial r}$ is almost independent of k_{ev} : $\overline{\partial C/\partial r}$ is determined by how much of the volatile component has evaporated, and it is independent how fast the volatile component has evaporated. Figure 4(d) and (e) shows that $C(r, t)$ at the edge quickly goes to zero when $RH = 0$, while the change of $C(r, t)$ in the droplet center is relative slow. As the average concentration gradient is mainly determined by the difference between the value of $C(r, t)$ in the droplet center and in the edge, the Marangoni flow is not strongly affected by k_{ev} . Therefore the change of $\theta(t)$ shown in Figure 4(a) is due to the effect of evaporation: evaporation decreases the contact angle as it is indicated by the last

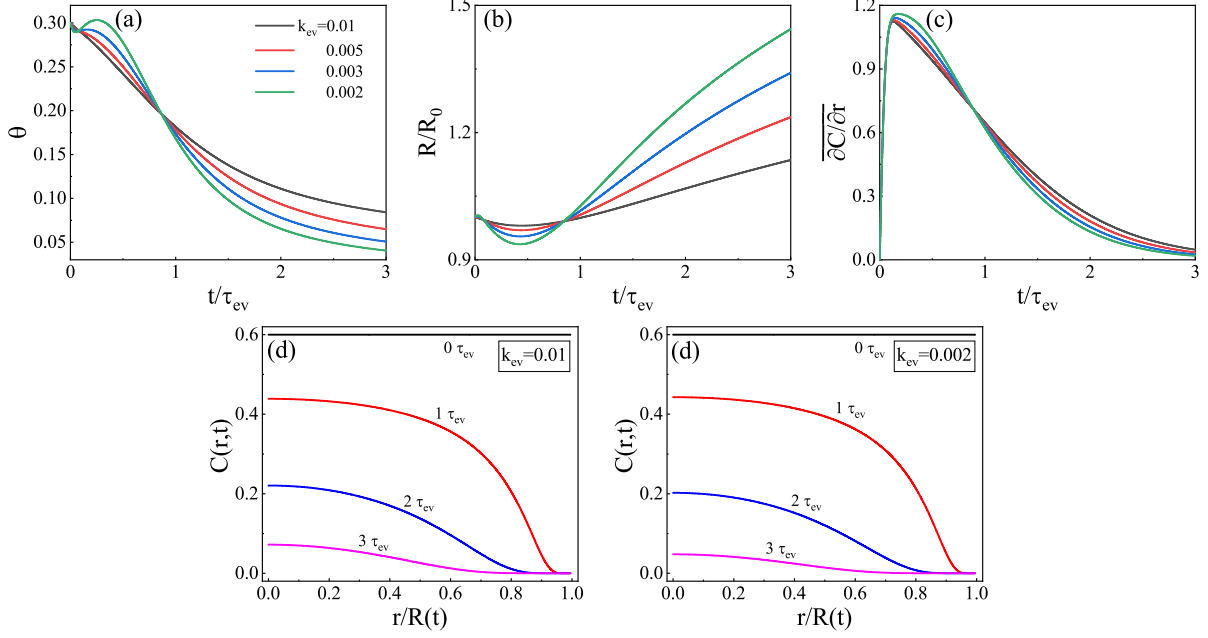


FIG. 4. Evolution of (a) droplet contact angle $\theta(t)$, (b) droplet contact radius $R(t)/R_0$, and (c) averaged concentration gradient $\overline{\partial C/\partial r}$ of an evaporating binary aqueous solution droplet for various values of k_{ev} . The evolution of the distribution of volatile component concentration within the droplet for (d) $k_{ev} = 0.01$, and (e) $k_{ev} = 0.002$. All other parameters are $RH = 0.0$, and $C_0 = 0.6$.

two terms on the right hand side of Eq. (A.35).

D. The values used for parameters

The justification for the values used for parameters in our calculations are provided as follows.

- (1) The evaporation rate parameter k_{ev} .

k_{ev} is defined by a ratio of two characteristic times, $k_{ev} = \tau_{re}/\tau_{ev}$, where $\tau_{re} = \eta V_0^{1/3}/\gamma_A$ and $\tau_{ev} = V_0/|\dot{V}_0|$. The time τ_{ev} represents the characteristic evaporation time for pure A droplet (of initial size V_0), and τ_{re} represents the relaxation time: the time needed for the pure A droplet (initially having contact angle θ_0) to have the equilibrium contact angle θ_e . The parameters η and γ_A are viscosity and surface tension of pure A droplet,

respectively. Due to the large difference between these parameters in different systems and conditions, the value range of k_{ev} is relatively large, and $k_{ev} \in [10^{-9}, 10]$ in general.

- (2) The relative surface tension γ_{re} .

Using the droplets made of propylene glycol (PG) and water, Cira et al. [9] observed the θ_{pk} phenomenon. The surface tension of water and PG in the experiment correspond to $\gamma_A = 73 \text{ mN m}^{-1}$ and $\gamma_B = 36 \text{ mN m}^{-1}$, respectively [9]. Put these parameters into $\gamma_{re} = \gamma_A/\gamma_B$, we have $\gamma_{re} \approx 2.03$. Thus we set $\gamma_{re} = 2$ in our calculations.

- (3) The initial contact angle θ_0 .

The error between $\cos \theta$ and $1 - \theta^2/2$ is within 0.5% when $\theta < \pi/6$. Moreover, the initial contact angle usually is set in between 0 – 0.5 in many other studies using lubrication approximation theory. For example, Williams et al. [8] set the initial aspect ratio $H_0/R_0 = 0.2$, which corresponds to $\theta_0 \approx 0.4$, where the evaporation of ethanol/water droplets was studied both experimentally and theoretically. Thus it is reasonable to set the initial contact angle $\theta_0 = 0.3$ in our calculations.

-
- [1] F. Parisse and C. Allain, Drying of Colloidal Suspension Droplets: Experimental Study and Profile Renormalization. *Langmuir*, 1997, **13**, 3598-3602.
- [2] A. D. Eales, N. Dartnell, S. Goddard and A. F. Routh, Thin, binary liquid droplets, containing polymer: an investigation of the parameters controlling film shape. *J. Fluid Mech.*, 2016, **794**, 200-232.
- [3] C. Diddens, J. G. M. Kuerten, C. W. M. van der Geld and H. M. A. Wijshoff, Modeling the evaporation of sessile multi-component droplets. *J. Colloid Interface Sci.*, 2017, **487**, 426-436.
- [4] M. Kobayashi, M. Makino, T. Okuzono and M. Doi, Interference Effects in the Drying of Polymer Droplets on Substrate. *J. Phys. Soc. Jpn.*, 2010, **79**, 044802.
- [5] X. K. Man and M. Doi, Ring to Mountain Transition in Deposition Pattern of Drying Droplets. *Phys. Rev. Lett.*, 2016, **116**, 066101.
- [6] M. Doi, *Soft Matter Physics*, Oxford University Press, 2013.
- [7] X. K. Man and M. Doi, Vapor-Induced Motion of Liquid Droplets on an Inert Substrate. *Phys. Rev. Lett.*, 2017, **119**, 044502.
- [8] A. G. L. Williams, G. Karapetsas, D. Mamalis, K. Sefiane, O. K. Matar and P. Valluri, Spreading and retraction dynamics of sessile evaporating droplets comprising volatile binary mixtures. *J. Fluid Mech.*, 2021, **907**, A22.
- [9] N. J. Cira, A. Benusiglio and M. Prakash, Vapour-mediated sensing and motility in two-component droplets. *Nature*, 2015, **519**, 446-450.